

Substrate involvement in dioxygen bond dissociation catalysed by iron phthalocyanine supported on Ag(100)

Francesco Sedona,^{*a} Matteo Lo Cicero,^{a,§} Silvia Carlotto,^a Andrea Basagni,^a Mir Masoud Seyyed Fakhrabadi,^{a,#} Maurizio Casarin,^a and Mauro Sambi^{*a, b}

a Department of Chemical Sciences, University of Padova, Via Marzolo 1, 35131 Padova, Italy. E-mail: francesco.sedona@unipd.it, mauro.sambi@unipd.it

b Consorzio INSTM, Unità di Ricerca di Padova, I-35131 Padova, Italy

§ Current address: School of Chemistry, Cardiff University, Park Place, Main Building, CF10 3AT Cardiff, U.K.

Current address: School of Mechanical Engineering, College of Engineering, University of Tehran, Tehran, Iran.

Electronic Supplementary Information

1. Experimental and computational details

STM and LEED experiments were performed in an Omicron variable temperature VT-STM system in UHV conditions. An Ag (100) single crystal (MaTeck GmbH) was cleaned by repeated cycles of 1 keV Ar⁺ sputtering and annealing at 820 K and used as the substrate. A few mg of FePc (Alfa Aesar GmbH, 95% purity) were loaded into a pyrolytic boron nitride (PBN) crucible connected to the preparation chamber and carefully degassed as described elsewhere¹. The Ag crystal was held at RT throughout the experiments. 1 ML of FePc is defined as a close-packed film of monomolecular thickness exhibiting the (7 0, 0 7) superstructure (that is, phase E). The resulting surface density is 0.345 nm².

Oxygen (Messer, 99.999% purity) was dosed at RT through a leak valve.

The STM measurements were carried out at RT in constant current mode, using a Pt-Ir tip obtained by electrochemical etching in aqueous solution. STM images were analysed with the WSXM software². Sample bias values are reported throughout the article.

Computational results on the relative stability of the B phase were obtained by means of periodic DFT calculations using the Quantum-ESPRESSO package.³ Wave functions relative to valence electrons were expanded on a plane-wave basis set with a kinetic energy cutoff of 27 Ry, while the interaction between valence electrons and ion cores was modeled by ultrasoft pseudopotentials.⁴ The cutoff on the charge density was 250 Ry. Spin polarised Kohn-Sham equation are solved with the generalised gradient approximation (GGA), adopting the Perdew-Burke-Ernzerhof (PBE)⁵ approximation. The Monkhorst-Pack method is adopted for the summation over the Brillouin zone, a 2x2 *k*-point mesh is used for the surface calculations, while a cold smearing⁶ of 0.02 Ry was applied to the electron population function. The distance between repeated images along the *z* direction was larger than 9 Å. The Ag(100) surface was modeled by a slab containing five atomic layers, the top three of which were allowed to relax and geometry optimisations were carried out with a convergence threshold of 10⁻⁴ Ry on the total energy. STM images were simulated within the

Tersoff-Hamann approach.⁷ Oxygen interaction with Ag (100)-supported FePc B ML phases was investigated using the same set-up.

2. Phase diagram of FePc/Ag(100) in the coverage range 0.9 – 1.0 ML

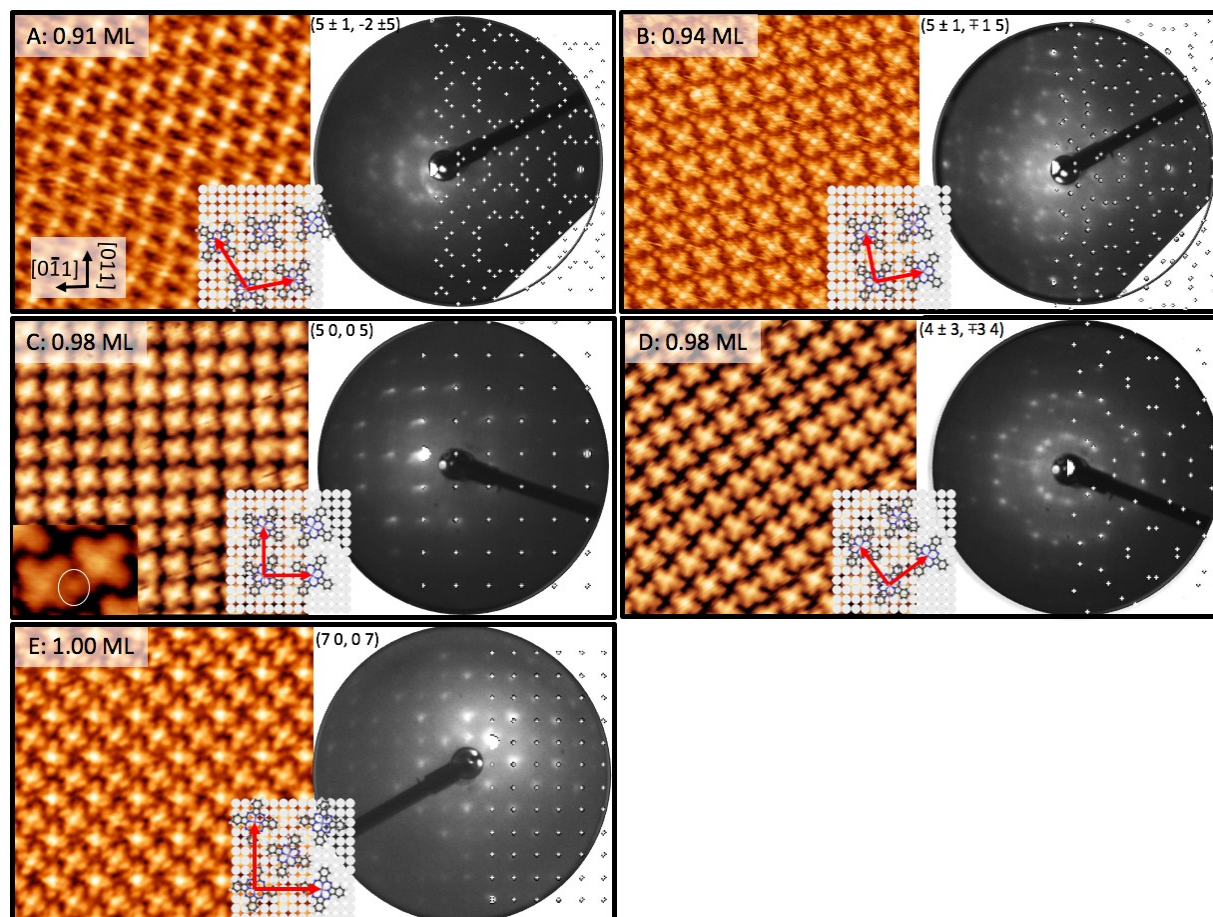


Fig. S1 STM images with surface coverage and matrix notations, unit cell models and LEED patterns with corresponding simulations of phase A ($13 \times 13 \text{ nm}^2$, $V = -0.6 \text{ V}$, $I = 3.78 \text{ nA}$); phase B ($13 \times 13 \text{ nm}^2$, $V = -0.5 \text{ V}$, $I = 2 \text{ nA}$); phase C ($13 \times 13 \text{ nm}^2$, $V = -0.2 \text{ V}$, $I = 3.9 \text{ nA}$); phase D ($13 \times 13 \text{ nm}^2$, $V = 0.5 \text{ V}$, $I = 0.75 \text{ nA}$) and phase E ($13 \times 13 \text{ nm}^2$, $V = -0.7 \text{ V}$, $I = 0.8 \text{ nA}$).

As easily deduced from the matrix notations, phases A and B have a common unit cell parameter of 14.73 \AA and are easily interconverted into each other by STM scanning along nearly horizontal molecular rows. At a coverage of 0.98 ML we observe the coexistence of two square phases commensurate with the substrate (C and D, respectively) and with the same lattice parameter of 14.45 \AA , but with different in-plane orientations.

In phases from A to D FePc molecules have the same azimuthal orientation with respect to the surface, making an angle of $15^\circ \pm 1^\circ$ between the axis bisecting the phenyl rings and the main directions of the substrate. The same orientation, which is independent on the chemical nature of the central atom, is reported for isolated transition metal phthalocyanines deposited on Ag(100).

Indeed, DFT simulations reveal that this rotation, allows the bond optimisation between the macrocycle aza-nitrogens and the surface Ag atoms, with the central metal atom placed on the Ag fourfold hollow site.⁸ Our DFT simulations performed on phase B confirm these results: the most stable configuration has the same azimuthal orientation found experimentally, with the central Fe atom on a hollow position. However, the energy difference with respect to the bridge site is below 0.1 eV (see below). Instead, due to the higher density, phase E is characterised by molecules with two different azimuthal orientations and two inequivalent (fourfold hollow and on-top) absorption sites (see STM image and model in Figure S1E).

3. STM of O₂ dosage on Phases B and C

Phase B

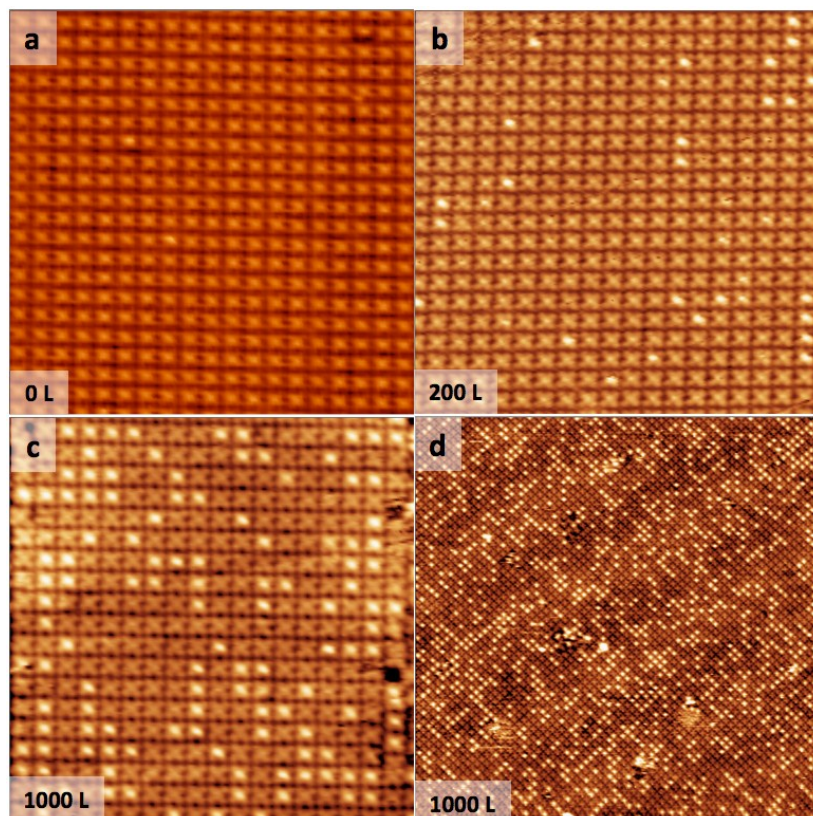


Fig. S2: STM images of phase B for increasing oxygen dosage at room temperature. a) 0 Langmuir (L) (30×30 nm², V=1.1 V, I=2 nA); b) 200 L (30×30 nm², V=0.6 V, I=12 nA); c) 1000 L (30×30 nm², V= 1 V, I=1 nA) and d) 1000 L (100×100 nm², V=0.8 V, I=6.5 nA).

Phase C

Movies **M1.mp4**, **M2.mp4** and **M3.mp4**, available as separately downloadable ESI files, show the behaviour of phase C upon O₂ dosing in the 0-1040 L range.

Movie **M1.mp4** shows the pristine data.

Movie **M2.mp4** highlights the FePc molecules reacting with oxygen. Continuous, dotted and double circles superimposed to each STM frame evidence the appearance, the disappearance, and the permanence of the reacted molecules with respect to the previous frame. Due to the STM drift, some molecules occasionally leave (enter) a frame with respect to the previous one. These molecules are highlighted with blue (red) circles and are not considered in the calculation of the percentages of reacting FePc molecules with respect to the total number of FePc units in the STM frame, which are reported in the histogram at the right of each frame.

In the histogram, the percentage of FePc \rightarrow FePcOx events is evidenced with yellow bars, the percentage of FePcOx \rightarrow FePcOx counts is highlighted by blue bars, the percentage of FePcOx \rightarrow FePc events is signalled by downward pointing black arrows, whose length is proportional to the percentage.

Movie **M3.mp4** evidences the intermolecular Ag adatoms. Light grey (yellow) dots highlight adatoms occupying a new (the same) position with respect to the previous STM frame. Adatoms occasionally leaving (entering) a frame due to the STM drift are highlighted in blue (red) and are not included in the calculation of the percentages of adatoms with respect to the total number of FePc molecules present in each frame, which are reported in the histogram to the right of the STM images.

In the histogram, the percentage of mobile (immobile) adatoms is represented by grey (yellow) bars.

4. Modeling the oxygen-FePc species

In this study, we first investigated the interaction of a single FePc with the Ag(100) surface for the B phase and we then considered the oxygen adsorption. To this end, three different adsorption sites are chosen by placing the Fe atom at, respectively, the top (top), hollow (hol) and bridge (brg) sites. The adsorption energy, E_{ads} , which accounts for the molecule-substrate interaction, is calculated through:

$$E_{ads} = E_{FePc + Ag} - E_{Ag} - E_{FePc}$$

where $E_{FePc + Ag}$ is the energy of the adsorbed FePc, E_{Ag} is the total energy of the Ag(100) surface and E_{FePc} is the energy of the isolated molecule frozen in the optimised geometry for the adsorbed species. The adsorption energies are -0.494 eV, -0.423 eV and -0.417 eV for hol, brg and top sites, respectively. A more negative adsorption energy indicates a stronger adsorption, but there is only a slight difference (below 0.08 eV) among the sites.

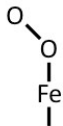
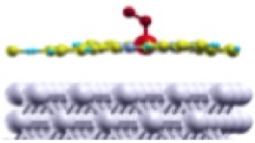
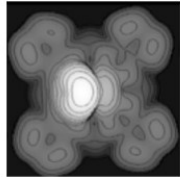
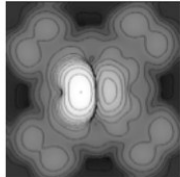
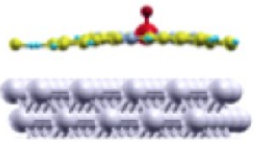
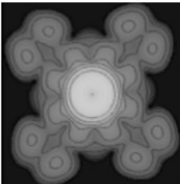
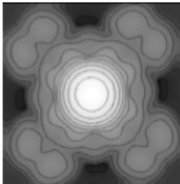
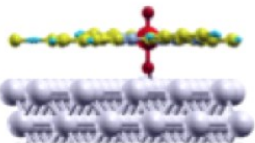
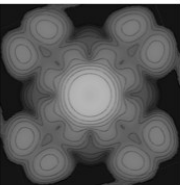
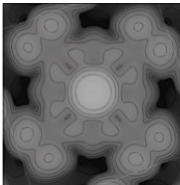
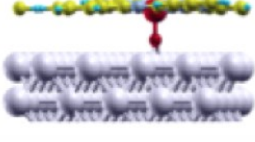
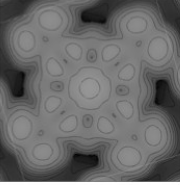
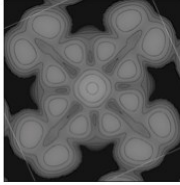
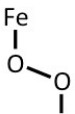
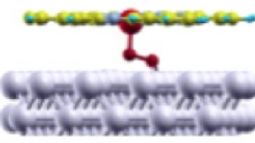
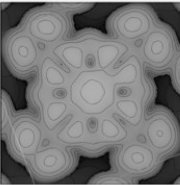
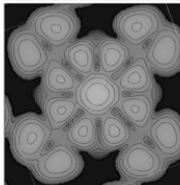
		Optimized structure	STM-TH (-1V)	STM-TH (+1V)
$(\eta^1\text{-O}_2)\text{-Fe-Ag}$				
O-Fe-Ag				
O-Fe-O-Ag				
Fe-O-Ag				
Fe-($\eta^2\text{-O}_2$)-Ag				

Fig. S3. Selected adsorption geometries of oxygen on the FePc-Ag(100) substrate. Simulated STM images are reported in the third and fourth columns for negative and positive bias, respectively, as computed by means of Tersoff-Hamann (TH) calculations.

Experimental data clearly show two different oxygen species adsorbed on Ag(100)-supported FePc. For this reason, several models were generated where oxygen, either in atomic or in molecular form, is placed in different ways on the FePc molecule and/or on the Ag surface (see Fig. S2). Our models were evaluated not on the basis of their stability, but rather on their ability to reproduce the experimental STM contrast and bias dependence. Of the investigated configurations, only $(\eta^1\text{-O}_2)\text{-Fe-Ag}$ and O-Fe-Ag are compatible with the experimental observations. Both these systems are strongly adsorbed on the Ag(100) surface with respect to FePc and their adsorption energies are -1.082 and -1.189 eV, for molecular and atomic oxygen systems, respectively.

6. References

1. M. Casarin, M. Di Marino, D. Forrer, M. Sambì, F. Sedona, E. Tondello, A. Vittadini, V. Barone and M. Pavone, *J. Phys. Chem. C*, 2010, **4**, 2144-2153.
2. I. Horcas and R. Fernández, *Rev. Sci. Instrum.*, 2007, **78**, 013705.
3. P. Giannozzi, S. Baroni, N. Bonini, M. Calandra, R. Car, C. Cavazzoni, D. Ceresoli, G. L. Chiarotti, M. Cococcioni, I. Dabo et al., *J. Phys. Condens. Matter*, 2009, **21**, 395502.
4. D. Vanderbilt, *Phys. Rev. B*, 1990, **41**, 7892-7895.
5. J. P. Perdew, K. Burke and M. Ernzerhof, *Phys. Rev. Lett.*, 1996, **77**, 3865-3868.
6. N. Marzari, D. Vanderbilt, A. De Vita and M. C. Payne, *Phys. Rev. Lett.*, 1999, **82**, 3296-3299.
7. J. Tersoff and D. R. Hamann, *Phys. Rev. Lett.*, 1983, **50**, 1998-2001.
8. A. Mugarza, R. Robles, C. Krull, R. Korytár, N. Lorente and P. Gambardella, *Phys. Rev. B*, 2012, **85**, 155437.